Journal of Luminescence 162 (2015) 191–196

Contents lists available at ScienceDirect

Journal of Luminescence

journal homepage: www.elsevier.com/locate/jlumin

Photoluminescence of indium-rich copper indium sulfide quantum dots

Wenyan Liu [a], Yu Zhang [a,b,*], Jia Zhao [a], Yi Feng [b], Dan Wang [b], Tieqiang Zhang [b], Wenzhu Gao [b], Hairong Chu [c], Jingzhi Yin [a], Yiding Wang [a], Jun Zhao [d,e], William W. Yu [a,d,e,*]

[a] State Key Laboratory on Integrated Optoelectronics, College of Electronic Science and Engineering, Jilin University, Changchun 130012, China
[b] State Key Laboratory of Superhard Materials, College of Physics, Jilin University, Changchun 130012, China
[c] Changchun Institute of Optics, Fine Mechanics and Physics, Chinese Academy of Sciences, Changchun 130025, China
[d] Department of Chemistry and Physics, Louisiana State University, Shreveport, LA 71115, United States
[e] College of Material Science and Engineering, Qingdao University of Science and Technology, Qingdao 266042, China

ARTICLE INFO

Article history:
Received 14 April 2014
Received in revised form
14 February 2015
Accepted 17 February 2015
Available online 25 February 2015

Keywords:
In-rich
Copper indium sulfide
Photoluminescence
Quantum dot

ABSTRACT

The enhanced photoluminescence (PL) for In-rich copper indium sulfide quantum dots (CIS QDs) was observed. The conduction electron-Cu vacancy recombination and the donor–acceptor pair (DAP) defect recombination were considered to exist in CIS QDs at the same time. The temperature-dependent PL study showed that the emission of these QDs might be mainly originated from the recombination between electrons in the quantized conduction band and holes in the copper vacancy acceptor when x was 0.500 ($Cu_xIn_{1-x}S$). However, the temperature coefficient of PL peak position decreased when x was 0.237. That meant the DAP recombination increased in the In-rich CIS QDs.

1. Introduction

There are numerous studies on the synthesis of semiconductor nanocrystals or quantum dots (QDs) due to their importance in optoelectronic, photovoltaic and biological applications [1]. Since the synthesis of monodisperse CdSe QDs by hot injection using organometallic precursors was reported [2], more work has been devoted to II–VI and IV–VI semiconductors, such as CdSe, CdS, CdTe, and PbS, PbSe, PbTe [3–7], due to their high quantum yield (QY) of fluorescence with tunable emission wavelength. However, toxic metals, such as Cd, Pb, and Hg, in the II–VI and IV–VI semiconductors, NCs have limited their possible applications. InP QDs have been regarded as the promising emitters covering blue to near-infrared (NIR). The covalent series of semiconductors are gradually increased, but the colloidal synthesis of this kind of nanocrystals is difficult [8]. InP QD's high-quality fluorescent properties have been demonstrated comparable to those of Cd-based QDs [9–12]. However, the synthesis of InP QDs may conflict with green chemistry principles because those high-quality InP QDs have to be achieved by using a highly expensive, toxic, unstable phosphorus (P) source of tris(trimethylsilyl)phosphine ($P(TMS)_3$). Besides, phosphides are known to be chemically less stable compared with sulfides [13] limiting their use in a viewpoint of practical application. As alternatives, ternary chalcopyrite-type I–III–VI group semiconductors with less-toxic components have been proposed [13–17].

Chalcopyrite semiconductors, such as $Cu(In/Ga)(S/Se)_2$, have been investigated mostly due to their potential in photovoltaic devices, especially for use in space stations, because they are very resistant to cosmic rays. In addition, the quantum structure of chalcopyrite semiconductors enables them to emit in the visible spectral range. Among them, CIS (the Bohr radius of exciton in CIS is ~4 nm [18]) seems to be a good candidate in the optical point of view, along with the requirement of Cd-free materials [14,19–23]. Recently, there have been some publications on the synthesis of CIS QDs and their luminescence properties [14,16,24–29]. Meanwhile, its composition-dependent optical properties have attracted more and more attentions due to the possible improvement of PL intensity, tunable band gap and further understanding of recombination in CIS QDs [30,31]. Omata et al. synthesized CIS QDs with an average size of 2.9–4.1 nm. They determined that PL emission was attributed to the recombination of electrons in the donor level and holes in the quantized hole state [32]. The authors proposed that the indium atom defects at copper sites or sulfur vacancies acted as donors at ~0.1 eV below the conduction band.

* Corresponding authors at: State Key Laboratory on Integrated Optoelectronics, College of Electronic Science and Engineering, Jilin University, Changchun 130012, China.
E-mail addresses: yuzhang@jlu.edu.cn (Y. Zhang), wyu6000@gmail.com (W.W. Yu).

http://dx.doi.org/10.1016/j.jlumin.2015.02.029
0022-2313/

Meanwhile, Kraatz et al. conclude that the optical transition responsible for the observed room-temperature PL in CIS/ZnS QDs originated from high-lying intraband donor states most likely associated with indium–copper antisite defects [33]. Recently, Cadirci et al. reported the ultrafast charge dynamics of CIS QDs using transient absorption spectroscopy [34]. It was confirmed that the cooling of hot photo-generated carriers to the band edge occurred within 3–5 ps. Kim et al. investigated the PL, Raman, and TRPL spectra of CIS QDs and concluded that the internal defect-related emission process was highly promoted by the large Cu deficiency, which was consistent with the improved PL intensity and the formation of defect-ordered structure by the large Cu deficiency in CIS QDs [35]. Chuang et al. synthesized $CuInS_2$/ZnS core/shell QDs with varying [Cu]/[In] ratios using a stepwise solvothermal route [36]. They studied the QY but without the analysis of temperature-dependent PL spectra of those CIS QDs. However, the research on detailed recombination mechanism in CIS QDs with different Cu/In ratios is still weak and we know such information is very important to establish the band structure model and to further improve the optical properties of CIS QDs. Meanwhile, the electron–hole recombination mechanism is the central issue for increasing the device efficiency, though CIS QDs have already been employed in several fields including solar cells [29] and light emitting diodes [37,38].

The change in the PL intensity as a function of temperature can often reflect the variation of the temperature-dependent non-radiative recombination centers or the evolution of the PL mechanism. In this work, we investigated the photoluminescence (PL) of In-rich CIS QDs, and achieved an 8 times enhanced PL efficiency. The temperature-dependent PL was employed to analyze the recombination processes in In-rich QDs.

2. Experiment

2.1. Chemicals

Indium (III) acetate ($In(Ac)_3$, 99.99%), oleic acid (OA, 99%) and 1-octadecene (ODE, 90%) were purchased from Alfa Aesar. Copper (I) iodide (CuI, 98%), zinc oxide (ZnO, 99.99%) and 1-dodecanethiol (DDT, 98%) were obtained from Aladdin Chemicals Co. Acetone, methanol, hexane, and toluene were purchased from Sigma-Aldrich. All chemicals were used directly without further treatment.

2.2. ZnO/OA/ODE solution

100.3 mg ZnO, 2.073 g OA and 10 mL ODE were loaded into a 25 mL three-necked flask. Then, the mixture was heated to 523 k until a colorless solution was achieved. The clear solution was cooled to 423 k for the next step.

2.3. Synthesis of CIS QDs with different Cu to In molar ratios ($Cu_xIn_{1-x}S$)

The synthesis of CIS QDs with $x=0.500$ was performed in a single flask. A mixture of 0.0376 g CuI (0.2 mmol), 0.0588 g $In(Ac)_3$ (0.2 mmol), 2 mL DDT and 8 mL ODE was loaded into a 50 mL three-necked flask. The reaction mixture was degassed under N_2 for 30 min. The flask was heated to 383 K for 4 h until a clear solution was achieved. The temperature was then raised to 503 K in 10 min. As the temperature increased, the color of the reaction solution progressively changed from colorless to yellow, then to red. 10 mL toluene was injected into the flask to quench the reaction when the temperature reached 503 K. In addition to the above CIS QDs using a precursor molar concentration ratio of Cu: In=1:1, the QDs with In-rich compositions were synthesized by using more amounts (0.4, 0.5, 0.6 and 0.8 mmol, corresponding to $x=0.435$, 0.294, 0.237, 0.227, respectively) of In precursor to prepare CIS QDs at the same reaction condition.

2.4. Synthesis of CIS/ZnS core/shell QDs with different Cu to In molar ratios ($Cu_xIn_{1-x}S$/ZnS)

In the above CIS QD synthesis, before the injection of toluene to quench the reaction, 12 mL ZnO/OA/ODE solution was injected into the solution at 503 K dropwise. The solution was maintained at this temperature for 2 h and was then cooled to 423 K for annealing (2 h).

Prior to the characterization and further experiments, the samples have to be purified to remove excessive reaction precursors and solvents, for which we resorted to our well-established purification approach. Hexane was added to the sample solution and methanol with twice volume was used for extraction [4,7,39]. The extracted CIS QDs were redispersed in hexane, then excess methanol and acetone were added to precipitate the QDs. Finally, the purified QDs were dispersed in solvents (e.g., toluene) for further measurements.

2.5. Characterization

Absorption spectra were measured on a Perkin-Elmer Lambda 950 UV–vis spectrophotometer. Photoluminescence (PL) spectra were measured on a Perkin-Elmer Luminescence LS50B spectrophotometer. The inductively coupled plasma (ICP) analyses were carried out on a Perkin-Elmer Optima 3300DV spectrometer. Transmission electron microscopy (TEM) observations were performed on a JEOL EM-2010F microscope operating at 200 keV. Samples for TEM studies were prepared by placing a 4 μL toluene solution of nanocrystals on ultrathin carbon-film-coated copper grids in a glove box. Time-resolved photoluminescence (TRPL) measurements were performed on a fluorescence spectrometer (mini-τ, Edinburgh Photonics) equipped with an EPL405 laser diode.

3. Results and discussion

According to the ICP analysis, CIS QDs with different x ($Cu_xIn_{1-x}S$, $x=0.500$, 0.435, 0.294, 0.237, and 0.227) were prepared. The PL spectra shown in Fig. 1a suggest that the PL emission of CIS QDs is related to copper deficiency. The CIS QDs with $x=0.237$ had a highest PL intensity.

Nam et al. [30] reported that the variations of optical band gap and emission peak energy versus different Cu to In molar ratios exhibited a tendency that the band gap and emission peak energy increased with a higher degree of Cu-deficiency. A similar evolution of the PL peak from 674.0 nm to 670.4 nm was observed when x varied from 0.500 to 0.227. Meanwhile, Fig. 1a indicates that the intensity of PL spectra increases with the concentration of In which is similar to the previous report [31]. After x varied from 0.500 to 0.237, the PL intensity was almost 8 times enhanced as shown in Fig. 1a. The increased In content resulted in more Cu-deficiencies and hence the increase of related defect concentration; these two factors made the PL intensity much stronger. The PL intensity decreased with the increasing copper deficient ($x<0.237$). The PL quenching of the CIS QDs with high concentration copper deficient might be caused by the interaction effects between defect states.

To analyze PL properties in-deep, the CIS QDs with $x=0.500$ and $x=0.237$ were chosen as samples *a* and *b*. Their absorption and PL spectra are shown in Fig. 1c. TEM photographs in Figs. 1d and 1e indicate that the particle sizes of samples *a* and *b* were

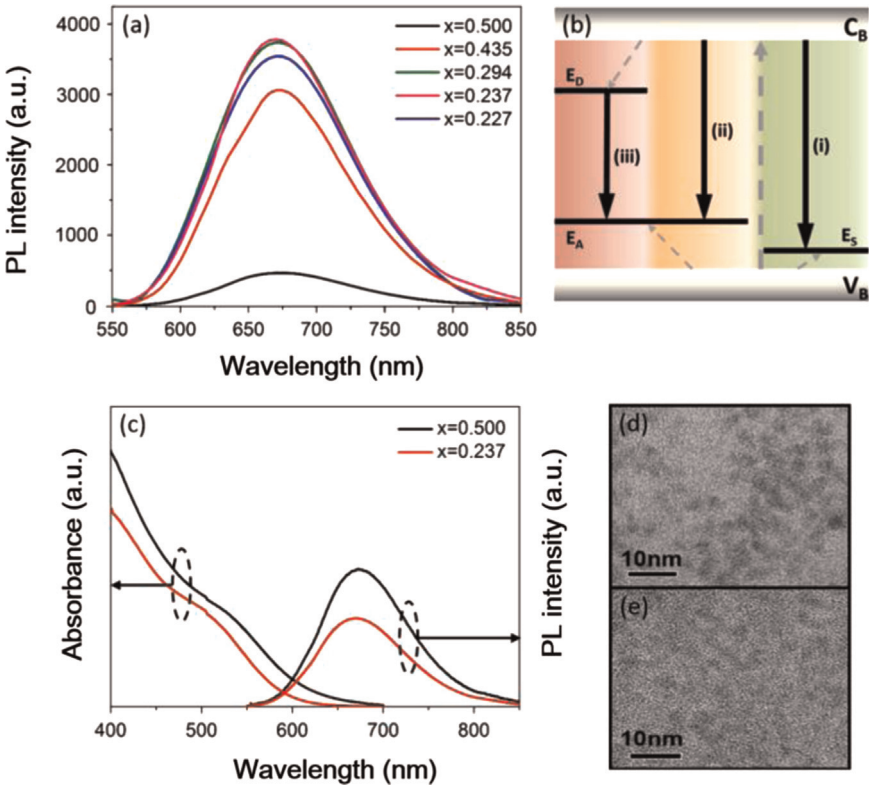

Fig. 1. PL spectra of $Cu_xIn_{1-x}S$ QDs with different x (a), schematic diagrams of the energy levels (b), absorption and photoluminescence spectra of CIS QDs at room temperature (c) and TEM photographs of CIS QDs ((d), $x=0.500$; (e), $x=0.237$).

2.7 nm and 2.3 nm, respectively. The broad absorption shoulders can be seen in Fig. 1c. The shoulders were attributed to the optical band gap, at which the electron–hole pair, i.e., the exciton, was generated. The absorption peaks of samples *a* and *b* were 546 nm and 530 nm, respectively. They were distinctly shorter than 800 nm that corresponds to the energy band gap of the bulk CIS (1.55 eV). The PL emissions were achieved in the visible region as shown in Fig. 1c. The emission peak widths of the present QDs were broad; this was consistent with the observation that the optical absorption shoulder was broadened as compared to that observed for CdSe QDs [40]. The emission peaks of samples *a* and *b* were 674 nm and 670 nm, and the full-width of the peak at half-maximum (FWHM) were ~111 nm and ~114 nm, respectively, which were significantly broader than those of high-quality CdSe QDs [41] but were similar to the $CuInSe_2$ QDs [42]. The wavelength differentials of absorbance and PL spectra of CIS samples *a* and *b* were 431 meV and 492 meV, respectively, which were too large to be attributed to a direct excitonic recombination because the differentials is at most 100 meV for excitonic recombination [2]. Such large differentials indicated that the emission should be attributable to the defect-related recombination.

According to the previous studies [43–48], sulfur vacancy (V_S), interstitial copper (Cu_i), and copper site substituted by indium (In_{Cu}) behave as donors, whereas copper vacancy (V_{Cu}), indium vacancy (V_{In}) and indium site substituted by copper (Cu_{In}) behave as acceptors in CIS. Several electronic transitions can be observed in PL among the defect levels, the conduction band (C_B), and the valence band (V_B); the observed emissions depend on the ratio of chemical compositions. In general, the transitions from C_B to V_{In} and/or Cu_{In} and from V_S and/or Cu_i to V_B are dominant for the Cu-rich composition, and the transitions from V_S to V_{Cu} and In_{Cu} to V_{Cu}, become significant and cannot be ignored for the In-rich composition [49].

In CIS QDs, the effective mass of electron is much smaller than that of hole. Therefore, the size-dependent increase in energy of the conduction band should be greater than that of the valence band. The increased energy of conduction band could be observed in process of emission with decreasing size. In other words, the energy of valence band was weakly dependent with size. According to the study of Nose et al. [49], the size-dependent shift of emission (320 meV) in $CuInSe_2$ QDs reached up to 71% of that in the optical band gap (450 meV). This size-dependent shift was observed in CIS QDs when the chemical composition was stoichiometric [16,37]. The size dependent shift of emission (121 meV) reached up to 75.2% of that in the optical band gap (161 meV) [16]. This proved that the shift from conduction band was 75.2%, which indicated that the emission should relate to conduction band. A time-resolved PL study showed that the PL lifetime of the ZnCuInS/ZnSe/ZnS QDs was a characteristic feature that dominated the transition from the conduction band to an acceptor level [50]. Therefore, the DAP recombination was not dominating for stoichiometric CIS QDs, but the conduction band-related transition was notable. It thus can be reasonably concluded that PL emission of CIS QDs involves three types of recombination at room temperature: surface-related recombination, C_B–V_{In} and/or C_B–Cu_{In} recombination, and donor–acceptor pair (DAP) defect recombination. Fig. 1b is a simulation of the process of recombination. E_A is the acceptor state, E_D is the donor state, and E_S is the surface state.

In order to further analyze the recombination states in these two CIS QDs, temperature-dependent PL spectra were measured. Fig. 2a and b shows the PL spectra of CIS QD samples *a* and *b* at a temperature range of 50–373 K. A red-shift and the peak broadening were observed with the increased temperature. Meanwhile, the decrease of PL intensity was observed. The energy of the defect states was weakly dependent on temperature. Therefore, the large variation of peak positions with temperature in PL spectra demonstrated that the dominated recombination might not be DAP recombination, but the electron–hole recombination from the C_B to acceptor levels for CIS QD samples *a* and *b*.

The changes of the peak position at different temperatures are shown in Fig. 2d. The PL peak of sample *a* with $x=0.500$ shifted from 665 nm to 683 nm, while the PL peak of sample *b* with In-rich composition varied from 664 nm to 676 nm. The temperature coefficient was smaller in In-rich CIS QDs (sample *b*). In chalcopyrite CIS, the bond strength of Cu–S bond is weaker than that of In–S bond, suggesting that the V_{Cu} forms preferably and accordingly causes the generation of anti-site defects [25,51]. For In-rich CIS QDs, the major defects can be V_{Cu}, In_{Cu}, and V_S [23,49,51] and their concentrations are high. Therefore, the increased concentrations of donor and acceptor caused the enhancement of DAP recombination that was weakly dependent on temperature. The increase of In composition induced the DAP recombination in CIS QDs [52]. The temperature dependent PL spectra of $Cu_xIn_{1-x}S$/ZnS QDs with $x=0.500$ (sample *c*) and $x=0.237$ (sample *d*) were also measured. The surface states were eliminated by introducing the shells. The changes of the normalized intensity and peak position at different temperatures are shown in Fig. 3. The decreased PL intensity of samples *c* and *d* were similar, which is the same to that of CIS QDs without shells. The PL peak of core/shell sample *c* with $x=0.500$ shifted from 609.5 nm to 627.7 nm, while the PL peak of sample *d* with In-rich composition varied from 612.2 nm to 622.3 nm as shown in Fig. 3b. The reduced temperature coefficient with increasing In compositions was the same to that of CIS QDs without shells. This result indicates that the increase of In composition caused the increase of donor and acceptor concentrations, which caused the enhancement of the weakly temperature dependent DAP recombination, and this enhancement was not related with surface states.

As shown in Fig. 2c, the data of temperature-dependence of the normalized PL intensities for $x=0.500$ and $x=0.237$ almost overlapped. According to the data, the variations of normalized PL intensity with different temperatures were similar in the two samples. In order to investigate the nonradiative relaxation process in QDs, we analyzed the temperature dependence of the normalized PL intensity. The PL intensities of CIS QDs with different x as a function of inverse K_BT are shown in Fig. 4. The PL intensity of the QDs decreased rapidly when temperature increased, and it could be attributed to the thermal activation and the thermal escape of carrier. The temperature dependence of the PL intensity can be described by the following equation [53]:

$$I_{PL}(T) = \frac{N_0}{1 + A\exp(-E_a/k_BT) + B[\exp(E_{LO}/k_BT) - 1]^{-M}} \quad (1)$$

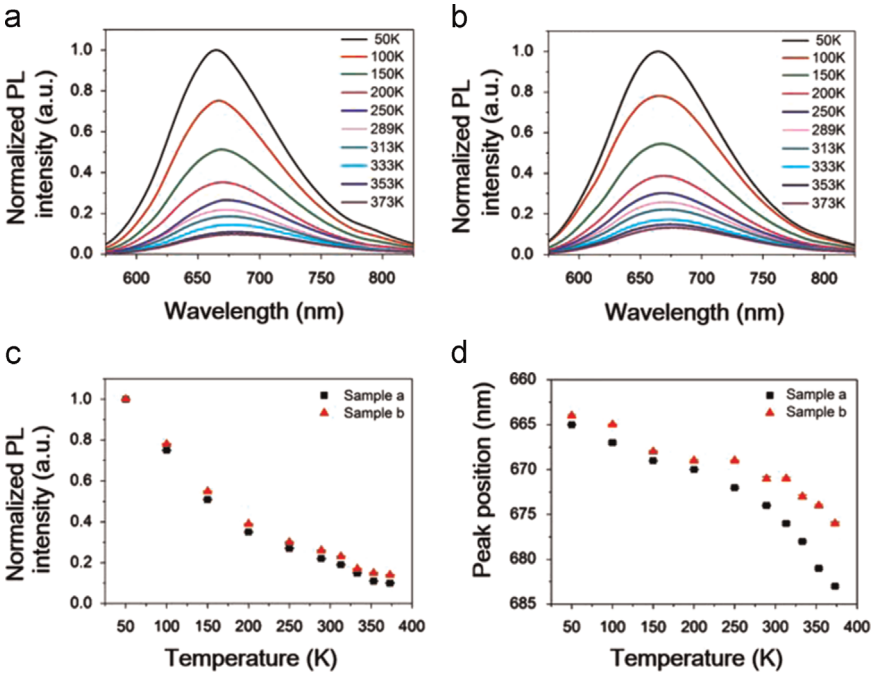

Fig. 2. Temperature dependent photoluminescence spectra of $Cu_xIn_{1-x}S$ samples *a* ($x=0.500$) and *b* ($x=0.237$) in the range of 50–373 K. Relationship of PL intensity (normalized) with temperature (c) and the evolution of PL peak position with temperature (d).

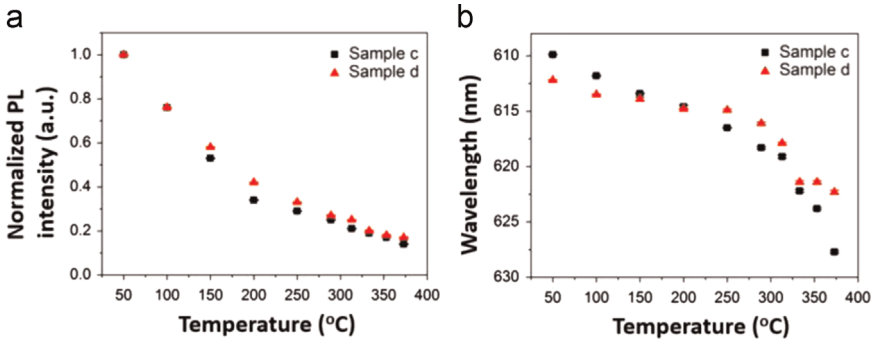

Fig. 3. Relationship of PL intensity (normalized) with temperature (a) and the evolution of PL peak position with temperature (b) of $Cu_xIn_{1-x}S$/ZnS samples *c* ($x=0.500$) and *d* ($x=0.237$).

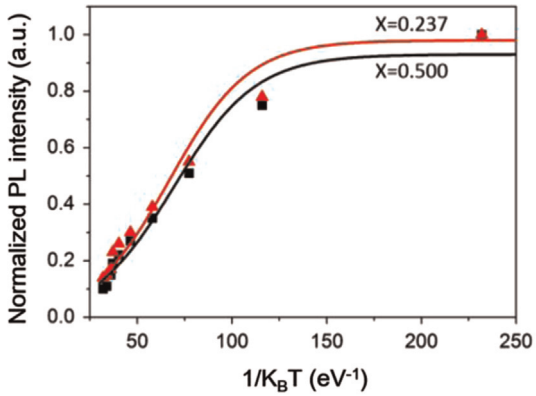

x	Ea (meV)	E_{LO} (meV)	m	A	B
0.500	46.5	35.1	4.2	25.5	5.5
0.237	48.1	35.0	4.1	25.5	5.5

Fig. 4. Normalized PL intensity of $Cu_xIn_{1-x}S$ QDs with different x as a function of $1/K_BT$ (top) and the fitting parameters (bottom). Solid lines are the fitting results according to Eq. (1).

where I_{PL} (T) is the integrated PL intensity at temperature T, N_0 is the initial carrier population of emitting states, E_a is the activation energy of surface defect states, m is the number of longitudinal-optical phonons for assisted thermal escape of carriers from dots, and A and B represent the ratios of the radiative lifetime in QDs and the capture time from emitting centers by nonradiative recombination centers. The parameters E_a, E_{LO}, and m for the samples of CIS QDs are summarized in Fig. 4 (bottom). In our previous study, the E_{LO} was determined to be 35.5 meV and 35.1 meV for ZnCuInS/ZnSe/ZnS QDs with the sizes of 2.7 nm and 2.3 nm, respectively. [50]. It is accordance with the E_{LO} from this work which was 35.1 meV for sample a and 35.0 meV for sample b. As shown in Fig.4, the fitting parameters of E_a, E_{LO}, and m were almost the same in CIS QDs with x=0.500 and x=0.237. Therefore, the interaction of carrier and phonon was similar in the different samples. In other words, the thermal activation and thermal escape of carrier were similar in CIS QDs with different Cu/In ratios, which indicated the similar energy structure of the two samples. In addition, this could be interpreted that the energy of an optical phonon was not to be strongly size-dependent [50] and component-dependent and it was the reason of the similar m. The nonradiative relaxation process with a small activation energy (40–50 meV) resulted in a decrease in the PL intensity. It is known that many defects such as V_{Cu} as acceptor and V_S, In_{Cu} as donors [32], resulting in recombination of a donor–acceptor pair and the conduction band-acceptor transition in the luminescence process in CIS QDs. Therefore, the PL of CIS QDs probably came from several kinds of recombination including the surface-related radiative recombination, the quantized conduction-band state to a localized intra-gap state recombination, and the DAP recombination. The x of CIS QDs ($Cu_{1-x}In_x$) varied from 0.500 to 0.237, the relative change of the different recombinations was caused by the change of V_{Cu}, V_S, In_{Cu}.

In order to further analyze the above results, the time-resolved PL spectra of CIS QDs with different Cu/In ratios have been measured. The time-resolved PL of CIS QDs is shown in Fig. 5. The long emission lifetime and the large differences between the PL band and the band-edge absorption feature, coupled with the observation of a size-dependence of emission wavelength [16,37], are inconformity with either strictly band-edge recombination or recombination between two localized states. Instead, they indicate that the radiative recombination in these NCs involves a transition

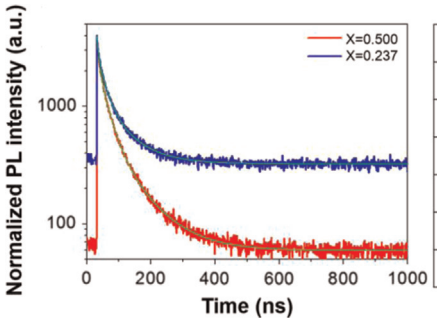

x	0.500	0.237
A_1	0.440	0.340
τ_1	33.633	27.643
A_2	0.424	0.457
τ_2	145.939	128.775
A_3	0.136	0.204
τ_3	470.035	417.711

Fig. 5. PL decay curves of $Cu_xIn_{1-x}S$ QDs (graph) and the fitting parameters (table).

from a quantized conduction-band state to a localized intra-gap state. The PL decays were not single-exponential, indicating the existence of several emission centers in the QDs. The decay traces of the samples were fitted with a tri-exponential function:

$$I(t) = A_1 \exp(-t/\tau_1) + A_2 \exp(-t/\tau_2) + A_3 \exp(-t/\tau_3) \quad (2)$$

where A_1, A_2 and A_3 were fractional contributions of PL decay lifetimes of τ_1, τ_2 and τ_3, respectively. The fitted results are shown in Fig. 4 (table), with τ_1 of 33.633 ns for sample a (x=0.500) and 27.643 ns for sample b (x=0.237), τ_2 of 145.939 ns for sample a and 128.775 ns for sample b, and τ_3 of 470.035 ns for sample a and 417.711 ns for sample b. According to the previous reports, the shorter lifetime (τ_1) may be due to the surface-related radiative recombination [16,54], the medium one (τ_2) may be due to the recombination a quantized conduction-band state to impurity level (defect state) [54,55], and the longer lifetime (τ_3) can be attributed to the DAP recombination [14,16,56]. The proportions of lifetime τ_2 and τ_3 for sample b (In-rich) were greater than that for sample a (x=0.500). And the proportion of lifetime τ_1 for sample b was smaller than that for sample a. The increased In content resulted in more Cu-deficiencies and hence the increase of related defect concentration. Related defects included the copper site substituted by indium (In_{Cu}) and copper vacancy (V_{Cu}) in In-rich QDs as discussed above. Therefore, the defect-related recombination could be enhanced including the near band-edge (from C_B to V_{Cu}) and DAP (from In_{Cu} to V_{Cu}) recombination. Comparing with the recombination from C_B to V_{Cu}, the contribution of DAP recombination increased dramatically while x decreased from 0.500 to 0.237. This could be confirmed by the increased proportions of A_2 and A_3 for sample b as shown in Fig. 5. And the ratio of A_3 (sample b/sample a) was 1.5, which was higher than that of A_2. As a result, the proportion of DAP recombination was boosted by the increase of In composition.

4. Conclusion

The ternary $Cu_xIn_{1-x}S$ QDs with different chemical compositions were prepared. There was possible defect-related multi-type recombination in CIS QDs: C_B–V_{In} and/or C_B–Cu_{In} recombination and DAP defects recombination resulted in the broad PL spectra and large Stokes shifts. The enhanced PL intensity of In-rich QDs was observed because of the increased concentration of In. The temperature-dependent PL was observed and was attributed to the recombination between electrons in the quantized conduction band and holes in the copper vacancy acceptor when x was 0.500. However, higher In composition would induce the DAP recombination in CIS QDs. Therefore, the temperature coefficient decreased when x changed to 0.237, because the temperature-independent DAP recombination was enhanced in In-rich CIS QDs.

Acknowledgment

This work was financially supported by the National Natural Science Foundation of China (61106039, 51272084, 61306078, 61225018, and 61475062), the National Postdoctoral Foundation (2011049015), the Jilin Province Key Fund (20140204079GX), the State Key Laboratory on Integrated Optoelectronics (IOSKL2012ZZ12), the Taishan Scholarship, the Shandong Natural Science Foundation (ZR2012FZ007), and NSF (1338346).

References

[1] M.G. Bawendi, M.L. Steigerwald, L.E. Brus, Annu. Rev. Phys. Chem. 41 (1990).
[2] C.B. Murray, D.J. Norris, M.G. Bawendi, J. Am. Chem. Soc. 115 (1993) 8706.
[3] J.E. Murphy, M.C. Beard, A.G. Norman, S.P. Ahrenkiel, J.C. Johnson, P. Yu, O.I. Mićić, R.J. Ellingson, A.J. Nozik, J. Am. Chem. Soc. 128 (2006) 3241.
[4] Y. Zhang, Q. Dai, X. Li, B. Zou, Y. Wang, W.W. Yu, J. Nanopart. Res. 13 (2011) 3721.
[5] W.W. Yu, X. Peng, Angew. Chem. Int. Ed. 41 (2002) 2368.
[6] W.W. Yu, J.C. Falkner, B.S. Shih, V.L. Colvin, Chem. Mater. 16 (2004) 3318.
[7] W.W. Yu, Y.A. Wang, X. Peng, Chem. Mater. 15 (2003) 4300.
[8] A.A. Guzelian, J.E.B. Katari, A.V. Kadavanich, U. Banin, K. Hamad, E. Juban, A.P. Alivisatos, R.H. Wolters, C.C. Arnold, J.R. Heath, J. Phys. Chem. 100 (1996) 7212.
[9] S. Hussain, N. Won, J. Nam, J. Bang, H. Chung, S. Kim, Chem. Phys. Chem. 10 (2009) 1466.
[10] L. Li, P. Reiss, J. Am. Chem. Soc. 130 (2008) 11588.
[11] E. Ryu, S. Kim, E. Jang, S. Jun, H. Jang, B. Kim, S.W. Kim, Chem. Mater. 21 (2009) 573.
[12] J. Ziegler, S. Xu, E. Kucur, F. Meister, M. Batentschuk, F. Gindele, T. Nann, Adv. Mater. 20 (2008) 4068.
[13] R. Xie, M. Rutherford, X. Peng, J. Am. Chem. Soc. 131 (2009) 5691.
[14] L. Li, T.J. Daou, I. Texier, T.T. Kim Chi, N.Q. Liem, P. Reiss, Chem. Mater. 21 (2009) 2422.
[15] K. Nose, Y. Soma, T. Omata, S. Otsuka-Yao-Matsuo, Chem. Mater. 21 (2009) 2607.
[16] H. Zhong, Y. Zhou, M. Ye, Y. He, J. Ye, C. He, C. Yang, Y. Li, Chem. Mater. 20 (2008) 6434.
[17] H. Zhong, Y. Li, M. Ye, Z. Zhu, Y. Zhou, C. Yang, Y. Li, Nanotechnology 18 (2007) 025602.
[18] H. Zhong, S. Lo, T. Mirkovic, Y. Li, Y. Ding, Y. Li, G.D. Scholes, ACS Nano 4 (2010) 5253.
[19] J. Krustok, J.H. Schon, H. Collan, M. Yakushev, J. Madasson, E. Bucher, J. Appl. Phys. 86 (1999) 364.
[20] H.W. Spiess, U. Haeberlen, G. Brandt, A. Räuber, J. Schneider, Phys. Status Solidi B 62 (1974) 183.
[21] H.Y. Ueng, H.L. Hwang, J. Phys. Chem. Solids 50 (1989) 1297.
[22] K. Wakita, F. Fujita, N. Yamamoto, J. Appl. Phys. 90 (2001) 1292.
[23] K. Wakita, H. Hirooka, S. Yasuda, F. Fujita, N. Yamamoto, J. Appl. Phys. 83 (1998) 443.
[24] S.L. Castro, S.G. Bailey, R.P. Raffaelle, K.K. Banger, A.F. Hepp, J. Phys. Chem. B 108 (2004) 12429.
[25] Y. Hamanaka, T. Kuzuya, T. Sofue, T. Kino, K. Ito, K. Sumiyama, Chem. Phys. Lett. 466 (2008) 176.
[26] H. Nakamura, W. Kato, M. Uehara, K. Nose, T. Omata, S. Otsuka-Yao-Matsuo, M. Miyazaki, H. Maeda, Chem. Mater. 18 (2006) 3330.
[27] K. Nose, N. Fujita, T. Omata, S. Otsuka-Yao-Matsuo, W. Kato, M. Uehara, H. Nakamura, H. Maeda, H. Kamioka, H. Hosono, J. Phys. Conf. Ser. 165 (2009) 012028.
[28] C. Xie, Y. Zhang, A.Y. Wang, W.W. Yu, J. Wang, J. Xu, MRS Proc. 1316 (2011) 03.
[29] L. Li, N. Coates, D. Moses, J. Am. Chem. Soc. 132 (2010) 22.
[30] D.E. Nam, W.S. Song, H. Yang, J. Colloid Interface Sci. 361 (2011) 491.
[31] B. Chen, H. Zhong, W. Zhang, Z. Tan, Y. Li, C. Yu, T. Zhai, Y. Bando, S. Yang, B. Zou, Adv. Funct. Mater. 22 (2012) 2081.
[32] T. Omata, K. Nose, K. Kurimoto, M. Kita, J. Mater. Chem. C 2 (2014) 6867.
[33] I.T. Kraatz, M. Booth, B.J. Whitaker, M.G.D. Nix, K. Critchley, J. Phys. Chem. C 118 (2014) 24102.
[34] M. Cadirci, O. Masala, N. Pickett, D. Binks, Chem. Phys. 438 (2014) 60.
[35] Y.K. Kim, S.H. Ahn, K. Chung, Y.S. Cho, C.J. Choi, J. Mater. Chem. 22 (2012) 1516.
[36] P.-H. Chuang, C.C. Lin, R.-S. Liu, ACS Appl. Mater. Interfaces 6 (2014) 15379.
[37] Z. Tan, Y. Zhang, C. Xie, H. Su, J. Liu, C. Zhang, N. Dellas, S.E. Mohney, Y. Wang, J. Wang, J. Xu, Adv. Mater. 23 (2011) 3553.
[38] Y. Zhang, C. Xie, H. Su, J. Liu, S. Pickering, Y. Wang, W.W. Yu, J. Wang, Y. Wang, J.I. Hahm, N. Dellas, S.E. Mohney, J. Xu, Nano Lett. 11 (2010) 329.
[39] Y. Zhang, Q. Dai, X. Li, Q. Cui, Z. Gu, B. Zou, Y. Wang, W.W. Yu, Nanoscale Res. Lett. 5 (2010) 1279.
[40] T. Omata, K. Nose, S. Otsuka-Yao-Matsuo, H. Nakamura, H. Maeda, Jpn. J. Appl. Phys. 44 (2005) 452.
[41] S. Taguchi, M. Saruyama, T. Teranishi, Y. Kanemitsu, Phys. Rev. B 83 (2011) 155324.
[42] P.M. Allen, M.G. Bawendi, J. Am. Chem. Soc. 130 (2008) 9240.
[43] F. Abou-Elfotouh, D.J. Dunlavy, D. Cahen, R. Noufi, L.L. Kazmerski, K. J. Bachmann, Prog. Cryst. Growth (1984) 365, Ch. 10.
[44] G. Dagan, F. Abou-Elfotouh, D.J. Dunlavy, R.J. Matson, D. Cahen, Chem. Mater. 2 (1990) 286.
[45] G. Masse, E. Redjai, J. Appl. Phys. 56 (1984) 1154.
[46] A.V. Mudryi, I.V. Bodnar, V.F. Gremenok, I.A. Victorov, A.I. Patuk, I.A. Shakin, Sol. Energy Mater. Sol. C 53 (1998) 247.
[47] P.W. Yu, J. Appl. Phys. 47 (1976) 677.
[48] S. Zott, K. Leo, M. Ruckh, H.W. Schock, J. Appl. Phys. 82 (1997) 356.
[49] K. Nose, T. Omata, S. Otsuka-Yao-Matsuo, J. Phys. Chem. C 113 (2009) 3455.
[50] W. Liu, Y. Zhang, W. Zhai, Y. Wang, T. Zhang, P. Gu, H. Chu, H. Zhang, T. Cui, Y. Wang, J. Zhao, W.W. Yu, J. Phys. Chem. C 117 (2013) 19288.
[51] M. Uehara, K. Watanabe, Y. Tajiri, H. Nakamura, H. Maeda, J. Chem. Phys. 129 (2008) 134709.
[52] H. Zhong, Z. Bai, B. Zou, J. Phys. Chem. Lett. 3 (2012) 3167.
[53] D. Valerini, A. Cretí, M. Lomascolo, L. Manna, R. Cingolani, M. Anni, Phys. Rev. B 71 (2005) 235409.
[54] L. De Trizio, M. Prato, A. Genovese, A. Casu, M. Povia, R. Simonutti, M.J. P. Alcocer, C. D'Andrea, F. Tassone, L. Manna, Chem. Mater. 24 (2012) 2400.
[55] L. Li, A. Pandey, D.J. Werder, B.P. Khanal, J.M. Pietryga, V.I. Klimov, J. Am. Chem. Soc. 133 (2011) 1176.
[56] T.K.C. Tran, Q.P. Le, Q.L. Nguye, L. Li, P. Reiss, Adv. Nat. Sci.: Nanosci. Nanotechnol 1 (2010) 025007.